



**HAL**  
open science

# Impact of La Niña on the Following-Summer East Asian Precipitation through Intermediate SST Anomalies

Na Wen, Laurent Li

► **To cite this version:**

Na Wen, Laurent Li. Impact of La Niña on the Following-Summer East Asian Precipitation through Intermediate SST Anomalies. *Journal of Climate*, 2023, 36 (17), pp.5743 - 5755. 10.1175/jcli-d-22-0650.1 . hal-04293704

**HAL Id: hal-04293704**

**<https://hal.science/hal-04293704>**

Submitted on 19 Nov 2023

**HAL** is a multi-disciplinary open access archive for the deposit and dissemination of scientific research documents, whether they are published or not. The documents may come from teaching and research institutions in France or abroad, or from public or private research centers.

L'archive ouverte pluridisciplinaire **HAL**, est destinée au dépôt et à la diffusion de documents scientifiques de niveau recherche, publiés ou non, émanant des établissements d'enseignement et de recherche français ou étrangers, des laboratoires publics ou privés.

# Impact of La Niña on the following summer East Asian precipitation through intermediate SST anomalies

Na WEN<sup>1\*</sup>, Laurent Li<sup>2</sup>

1. Center for Ocean-Atmosphere Interaction Research (COAIR) and College of Atmospheric Sciences, Nanjing University of Information Science and Technology, Nanjing, China
2. Laboratoire de Météorologie Dynamique, CNRS, Sorbonne Université, Ecole Normale Supérieure, Ecole Polytechnique, Paris, France

Journal of Climate, accepted (2023-04-27) <https://doi.org/10.1175/JCLI-D-22-0650.1>

Corresponding author address: Dr. Na Wen, College of Atmospheric Sciences, Nanjing University of Information Science & Technology, Nanjing 210044, China, E-mail: [wenna@nuist.edu.cn](mailto:wenna@nuist.edu.cn)

**Abstract:** This study investigates the impact of boreal winter-peaked La Niña on the following summer precipitation in East Asia through intermediate SST (Sea-Surface Temperature) anomalies playing the role of relay, in observation and numerical models. There are widespread dry conditions in both North and South China, and wet conditions in coastal areas of central and eastern China. Such a pattern is mainly attributed to an anomalous low pressure over the western tropical Pacific and an anomalous anticyclone over Northeast Asia. It is found that the delayed impact of La Niña on East Asian climate is operated through intermediate SST anomalies - the Z-shape cold SST anomalies in the tropical - North Pacific. There might be three ways for the SST anomalies to operate. Firstly, they produce tropical atmospheric perturbations that can penetrate into the subtropical jet through the westerly trough over the northeast subtropical Pacific, the wave train being then excited along the jet. Secondly, perturbations created through the monsoon trough over the western Pacific can directly stimulate northward propagating Rossby waves along the East Asian coast, mainly at low level. And thirdly, perturbations over the tropical Atlantic - Northwest Africa can also trigger downstream propagating waves along the subtropical jet. The observation effects of the intermediate SST anomalies and their possible impact mechanisms on atmospheric circulation are largely reproduced within numerical simulations performed with the Community Earth System Model.

## 1. Introduction

El Niño – Southern Oscillation (ENSO) is the most remarkable phenomenon in the tropical Pacific at interannual time scale, and has a huge amount of influence on global climate. Its positive phase, El Niño, attracts a lot of scientific interest and public awareness. El Niño exerts influences not only in its peak time in boreal winter, but also in its decaying stage in the subsequent summer (Rasmusson and Carpenter, 1982; Ropelewski and Halpert, 1987). As a regional manifestation, East Asia shows excessive precipitation in the middle and lower reaches of the Yangtze River in summer following El Niño (Zhang et al. 1999; Chang et al. 2000; Wang and Zhang 2002; Wu et al. 2009). Since sea surface temperature (SST) anomalies directly related to El Niño are largely reduced or even entirely disappear in the following summer, intermediate players must intervene to relay effects of winter-peaked El Niño. That's because the atmospheric response to underlying surface anomalies is very fast, within only a few days or weeks (Hoskins and Karoly, 1981; Peng and Whitaker, 1999; Li and Conil 2003), and the East Asian summer monsoon change can only be a quasi-simultaneous response to summer SST anomalies. Several hypotheses, which all used intermediate SST anomalies in the other oceanic basins to explain the delay effect of El Niño, were proposed in the literature, such as those involving local air-sea interaction sustaining the Philippine Sea anticyclone (PSAC) (Wang et al., 2002, 2003), the 'recharge and discharge' effect of the

tropical Indian Ocean (Yang et al., 2007; Xie et al., 2009), and the possible bridging role of the tropical Atlantic SST anomalies (Rong et al., 2010).

La Niña is the antiphase of El Niño in the ENSO cycle, but not its simple mirror. There are asymmetries in many aspects, such as amplitude, event evolutionary course and associated atmospheric responses (Zhou et al., 2004; McPhaden and Zhang, 2009; Dommenges et al., 2013; Okumura, 2019). The center of La Niña SST anomaly is usually westward shifted, relative to that of El Niño, and with weaker amplitude (Kang and Ku, 2002). This was believed to be the consequence of SST nonlinear advection in the equatorial eastern Pacific (An and Jin, 2004; Su et al., 2010) or nonlinear atmospheric processes including the asymmetrical wind stress feedback over the equatorial central Pacific (Kang and Ku, 2002; Choi et al., 2013) and stochastic forcing exerted on the ocean-atmosphere coupled system (Eisenman et al., 2005; Rong et al., 2011). Actually, the dependency of atmospheric deep convection on the underlying SST conditions (Gadgil et al., 1984) provides the most evident nonlinearity, convection anomalies during La Niña being largely displaced westward relative to El Niño. As a result, the associated atmospheric circulation responses in the Northern Hemisphere are approximately shifted by 35 degrees of longitude in phase (Hoerling et al., 1997). Similarly, Wu et al. (2010) demonstrated that the anomalous cyclone over the Philippine Sea during the mature phase of La Niña tends to shift westward, compared with its anticyclonic counterpart during El Niño. It is also noted that the nonlinear response over the Philippine Sea can lead to asymmetrical evolution of La Niña and El Niño (Ohba and Ueda, 2009). Chen et al. (2016) showed that the asymmetric wind stress in the far western tropical Pacific, which is associated with the Philippine cyclone, exerts a distinctive impact on the thermocline evolution at the decaying stage of La Niña. Consequently, La Niña usually displays a weaker decay after its peak and a regain of intensity in the following winter, while El Niño shows a rapid decay and a fast phase transition (Okumura and Deser, 2010).

Due to these distinctive features of La Niña, its delayed effect on the subsequent summer monsoonal rainfall in East Asia deserves a comprehensive investigation. The questions to be addressed are the following: How does La Niña influence the following summer precipitation over East Asia? What is the intermediate SST anomaly in its delay effect? How is the case of La Niña different from El Niño? One further remark needs to be made here about the diversity of ENSO. Based on the spatial location of anomalous SST in the tropical Pacific, El Niño events can be classified into different types (Ashok et al., 2007; Kao and Yu., 2009; Kug et al., 2009), and the following summer precipitation response over East Asia strongly depends on the types of El Niño (Wen et al., 2022, hereafter referred to as WLH22). Actually, precipitation anomalies are tightly linked to different intermediate SST anomalies from other oceanic basins while El Niño decays in the tropical Pacific. However, the classification of La Niña events has so far been controversial. Kug and Ham (2011) found the cold events of the ENSO cycle are highly correlated across the central and eastern Pacific, and therefore it is difficult to define prominent types for La Niña. Although Shinoda et al. (2011) separated a certain pattern of La Niña Modoki from normal events with satellite observation, there are very few cases that can be identified. Yuan and Yan (2013) tried to separate the influence of EP (Eastern Pacific) La Niña on the tropical atmosphere from that of CP (Central Pacific) type (for which SST anomaly is over the central - eastern equatorial Pacific). But there are much less EP La Niña cases that can be identified in mature-phase winter. Using the joint Self-Organizing Map (SOM) analysis, Ashok et al. (2017) also confirmed that types of La Niña are less distinguishable than those of El Niño. In short, there is still a lot of uncertainty about the classification of La Niña, but it is doubtless that SST anomalies of most La Niña cases, particularly the strong ones, are located in the central and eastern equatorial Pacific.

In present work, we mainly investigate the influence of strong La Niña on East Asian precipitation in the following summer and search any intermediate SST anomalies that can

sustain the delay effect. The paper is organized as follows. Section 2 describes the data and method used. The impact of La Niña on East Asian precipitation in the following summer and the associated regional circulation anomaly are presented in section 3. In section 4, the intermediate SST anomalies which relay the winter La Niña effect into the following summer are identified. Furthermore, the possible mechanisms for the impact of SST anomaly on atmosphere are also investigated. The observed results are further confirmed by modelling experiments in section 5. Section 6 gives the summary and discussion.

## **2. Data and methods**

### **a. Observational data and diagnostic method**

The observation and model data used in this study are the same as in WLH22. For the sake of completeness, we here give a short description. The precipitation is from the Chinese Meteorological Data Center, China Meteorological Administration, with a study area (east of 100°E) including 140 stations over East China. To avoid the effect of a strong interdecadal shift taking place at the end of 1970s, the time period of our investigation is taken from 1979 to 2021. The percentage of precipitation anomaly, which is the ratio of the anomalous precipitation to its seasonal climatological mean, is used to represent its variability. To reduce noises, the precipitation was reconstructed using the first leading empirical orthogonal function (EOF) mode that retains 70% of the total variance. The monthly sea-surface temperature (SST) and atmospheric variables in the same period are from the National Centers for Environmental Prediction-National Center for Atmospheric Research (NCEP-NCAR) reanalysis data (Kalnay et al. 1996) at a grid of 2.5° X 2.5°. All variables are deduced from their mean seasonal cycles and long-term trends.

The composite method is used in this study with Student's t-test (two-tail) for evaluating statistical significance. Strong La Niña cases in boreal winter (three-month mean of December, January and February, DJF0) are selected for the composite analysis based on Niño 4 index, where the SST anomaly in the region (5°S-5°N, 160°E-150°W) is beyond one negative standard deviation. Nine events are selected from 1979 to 2021 (1988/1989, 1998/1999, 1999/2000, 2000/2001, 2007/2008, 2008/2009, 2010/2011, 2011/2012 and 2020/2021). Through a case-by-case examination, we find that the evolution of the SST anomaly of 2008/2009 La Niña and the atmospheric response are very different from other events. To improve the signal-to-noise ratio, we removed this event from the composite analysis. It is to be noted that main conclusions presented in the paper are unchanged, if all La Niña cases during a longer period (1958~2020) are used following the criteria established by the Climate Prediction Center (CPC, [https://origin.cpc.ncep.noaa.gov/products/analysismonitoring/ensostuff/ONI\\_v5.php](https://origin.cpc.ncep.noaa.gov/products/analysismonitoring/ensostuff/ONI_v5.php)).

To investigate the physical mechanism explaining the role of the intermediate SST anomalies in the delay effect of La Niña on atmospheric circulation, as in Wen et al. (2020), we also calculate the wave activity flux as defined by Takaya and Nakamura (2001). The wave activity flux is parallel to the group velocity of the stationary Rossby wave embedded in the mean flow.

### **b. Model and experiment**

To confirm the physical mechanisms deduced from the observation, we leverage the results of existing model experiments, such as the Global Ocean Global Atmosphere (GOGA) and the Pacific pacemaker experiments (Deser et al., 2017) which were performed by the Climate Variability and Change Working Group (CVCWG, NCAR) using the Community Earth System Model (CESM1.1). The GOGA experiment was conducted using the observational SST and sea-ice forcing (NOAA Extended Reconstruction Sea Surface

Temperature version 4, ERSSTv4), with CAM5 (Community Atmosphere Model, version 5), the atmospheric component of CESM1.1. The simulation comprises 10 members of different initial conditions, but all from 1880 to 2014. The Pacific pacemaker experiment comprises 20 members with CESM1.1. In this pacemaker experiment, the temporal evolution of the eastern tropical Pacific SST ( $10^{\circ}\text{S}$ – $10^{\circ}\text{N}$ ,  $160^{\circ}$ – $90^{\circ}\text{W}$ , with a buffer zone extending to  $20^{\circ}\text{S}$  and  $20^{\circ}\text{N}$ , and  $180^{\circ}\text{W}$  to the American coast) is nudged to observations during 1920–2013 (ERSSTv4). This nudging operation maintains the observed evolution of ENSO, while the rest of the coupled system is free to evolve. We use the ensemble mean and process the model output in the same way as we do for observations. Noticing that the 2020/2021 La Niña case is missing in CESM due to its earlier ending of experiment, but our conclusion remains robust if we also exclude the 2020/2021 case from our observation diagnosis.

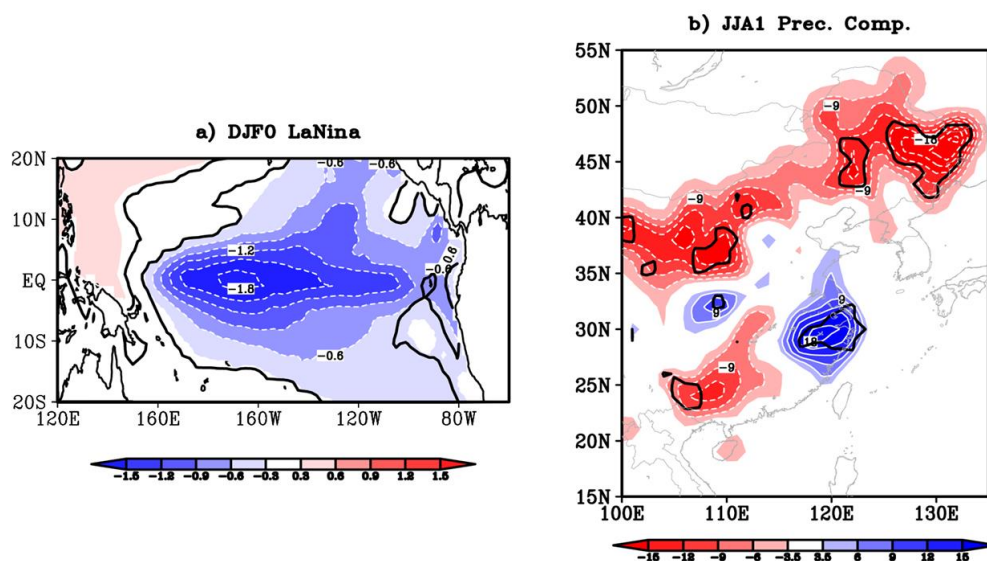


**Figure 1** a) Composite sea-surface temperature (SST) anomaly for La Niña in winter (DJF0, December–January–February, Contour interval (CI)  $0.3^{\circ}\text{C}$ ). Events are selected based on Niño-4 index, where the SST anomaly is beyond a negative standard deviation  $5^{\circ}\text{S}$ – $5^{\circ}\text{N}$ ,  $105^{\circ}$ – $180^{\circ}\text{W}$ . b) Corresponding precipitation anomaly over East Asia (CI=3%) in its decaying summer (JJA1, June–July–August). The thick black contour denotes the 90% confidence level for precipitation, but 95% confidence level for SST anomalies.

### 3. Impact of La Niña on East Asian climate

As shown in Fig. 1a, the main body of La Niña is ellipsoidal, mainly covering the Niño-4 and Niño-3.4 regions. Compared to the strong El Niño (typically EP El Niño, such as shown in Fig. 1a of WLH22), SST anomaly of La Niña is slightly narrower and longer, with the anomalous center westward shifted. The maximal amplitude of SST anomaly (Fig. 1a) is only  $1.5^{\circ}\text{C}$ , which is much smaller than that of El Niño. These features are consistent with the fact that La Niña and El Niño are generally opposite in sign, but show strong asymmetry (Su et al. 2010; Song et al., 2022). The corresponding precipitation anomalies in the following summer show widespread dry conditions over northern and northeastern China. The amplitudes are around 10~20% of the summer mean precipitation, which pass the 90% confidence level. There are also significantly positive precipitation anomalies along the eastern coast of China, and slightly negative precipitation anomalies over southern China (Fig. 1b). This anomalous level, smaller than the counterpart of El Niño (Fig. 1 in WLH2022), reveals the relative weak influence of La Niña on the following summer precipitation over East Asia. The precipitation pattern is also quite different from that of El Niño, which indicates a different physical mechanism of La Niña influence on the East Asian climate in

the following summer.

The precipitation anomaly over East Asia (Fig. 1b) is mainly attributed to an anomalous cyclone over the western tropical Pacific and anomalous high pressure over Northeast Asia. As shown in Fig. 2a, there is a pronounced cyclone at 500-hPa with an anomalous center over the South China Sea. It resembles the anti-phase of the Philippine Sea anticyclone (Wang et al., 2002), which causes the Western Pacific Subtropical High to retreat eastward by 10 degrees of longitude (as indicated by the dark red dash line in Fig. 2a). In addition, anomalous high-pressure anomaly is situated in Northeast Asia. The low pressure in the south and the high pressure in the north create the anomalous easterlies between them, blowing from the western Pacific to eastern-central China. This results in the convergence of water vapor at the junction of land and sea, which corresponds to the precipitation anomalies mainly in the east coast of China (Fig. 2c). However, most areas in north and northeast China are in the control of anomalous high pressure. The anticyclone-induced subsidence causes the region unusually dry, as indicated by the red shading in Fig. 2b. For southern China, on the northwest flank of the anomalous cyclone, anomalous northeasterly winds prevail (Fig. 2c). Cold and dry airs lead to dry conditions there. Therefore, the cyclone over the western tropical Pacific and the anticyclone over Northeast Asia are the key circulations for the precipitation anomaly in Fig. 1b.

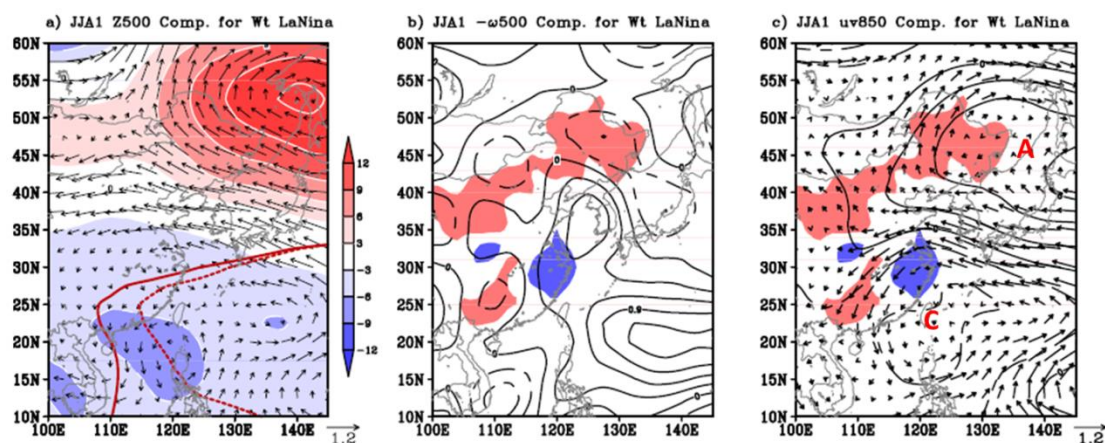


**Figure 2** Composite atmospheric circulation anomalies over East Asia in La Niña-decaying summer. a) 500- hPa geopotential height (shading, CI=3 m) and wind (vector, unit: m/s). The composite (climatological) Western Pacific Subtropical high is denoted by the 5860 m geopotential height with thick red dashed (solid) line. b) 500- hPa vertical velocity ( $-\omega$ ) (CI= $0.3 \times 10^{-2}$  Pa/s). c) 850- hPa geopotential height (black contours, CI=2 m) and wind (vector, unit: m/s). The red letters “C” and “A” mark the cyclones and anticyclones respectively. The shadings in b) and c) indicate the precipitation anomalies as in Fig. 1b, with blue (red) for precipitation anomalies greater (less) than  $\pm 6\%$ .

#### 4. Intermediate SST anomalies sustaining La Niña delay effect

The subsequent question to address is how winter-peaked La Niña impacts East Asian summer precipitation while it is at its decaying stage with original SST anomalies in the equatorial Pacific very much damped. To address the question, we first use observation data to detect potential intermediate SST anomalies in relation to La Niña in observation, and then investigate the physical mechanisms by which SST anomalies impact the atmosphere.

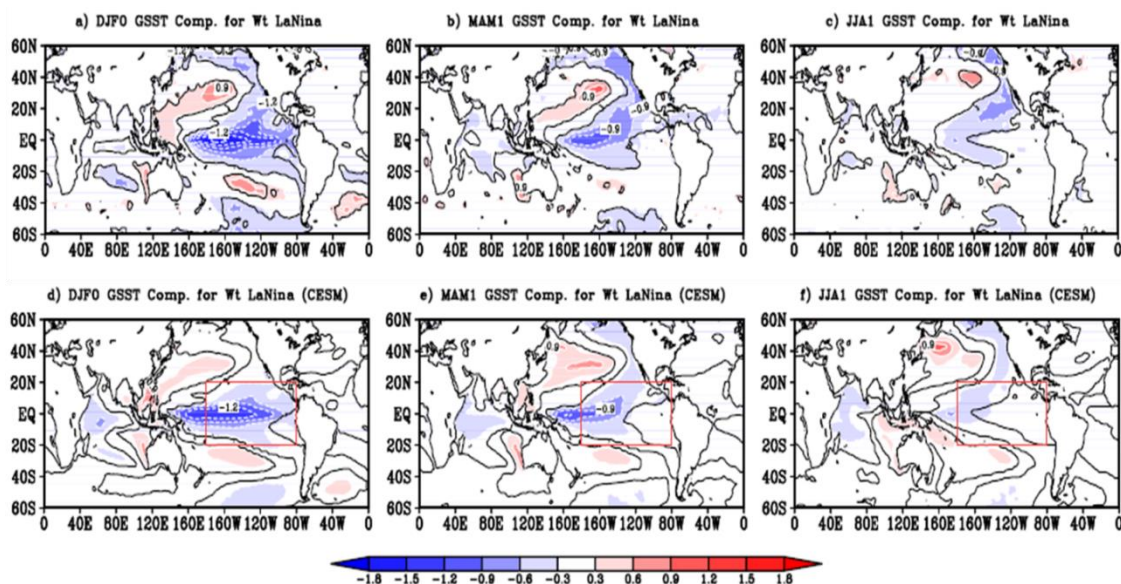


**Figure 3** Evolution of the composite SST anomalies ( $CI=0.3^{\circ}C$ ) for La Niña from its mature winter (DJF0, left panels), through the following spring (MAM1, March, April and May, middle panels), to the decaying summer (JJA1, right panels). The upper panels are derived from NCAR-NCEP reanalysis data, while the bottom panels are for the Pacific pacemaker experiment of the Community Earth System Model (CESM). The thick black contour denotes the 95% confidence level. In the bottom panels, the red box indicates the region ( $20^{\circ}S-20^{\circ}N$ ,  $180^{\circ}-80^{\circ}W$ ) where SST anomalies are nudged to ERSSTv4 observation.

#### a. Seasonal evolution of SST anomalies and atmospheric response

Figure 3 displays the evolution of global SST anomalies at La Niña's different stages. Intermediate SST anomalies that can relay the winter La Niña effect into the following summer are probably located over the tropical-North Pacific. As shown in Fig. 3a, b and c, the most pronounced behavior is the evolution of SST anomalies along the west coast of North America. In the mature-phase winter, a narrow zone of cold SST, which is connected to the main body of La Niña in the eastern-central tropical Pacific, propagates northward along the west coast of North America (Fig. 3a). It is strengthened in the subsequent spring, while the main body of La Niña is weakened westward with the anomaly center over the central tropical Pacific (Fig. 3b). In the following summer, the coastal SST anomaly of North America merges with the residual La Niña SST anomaly and forms a prominent Z-shape pattern across the tropical-North Pacific (Fig. 3c), which provides a possible 'bridge' to connect the winter La Niña with the following summer precipitation in East Asia. The La Niña - associated SST anomaly along the west coast of North America in Fig. 3a, b and c is probably due to the adjustment of polarward coastal Kelvin waves (Chelton, 1982) or atmospheric forcing over the tropical-North Pacific (Mantua et al., 1997; Schwing et al., 2002). The slightly amplified SST anomalies in the northeast subtropical Pacific (off the coast of California) may also involve local air-sea interactions (Vimont et al., 2002). Besides SST anomalies in the northeast subtropical Pacific, La Niña also induces cold SST anomalies in the tropical Indian Ocean at the mature phase (Fig. 3a). They strengthen in the following spring, but almost disappear in the following summer (Fig. 3b and c). Therefore, the tropical Indian Ocean has minor contribution to the relation of winter-peaked La Niña with the East Asian precipitation in the following summer. Similar results are observed in other oceans, e.g. the SST anomalies in the tropical North Atlantic. Such a configuration suggests that La Niña might mainly rely on the Z-shape SST anomaly in the tropical-North Pacific to convey its delayed effect.

Corresponding to such intermediate SST anomalies, the atmospheric circulation at upper level shows a low-pressure belt in the tropics and a clear wave train in mid-latitudes. As displayed in Fig. 4a, the entire tropics are dominated by low pressures with an asymmetric pair of Rossby waves across the eastern-central equatorial Pacific at 200-hPa. The larger lobe in the Northern Hemisphere extends its low-pressure anomaly eastward to the northern subtropical Atlantic. Consistent with what observed at upper level, the atmospheric circulation at 850-hPa shows a clear divergence over the eastern-central tropical Pacific, which results in a descending motion in the middle troposphere and surrounding ascents over the western tropical Pacific and equatorial Atlantic respectively (Fig. 4b). The configuration of the circulations between upper and low levels is in line with the atmospheric response to the asymmetric heating about the equator (Gill, 1980).

Compared with the tropics, the mid-high latitude atmospheric response is a clear wave train at upper level with pronounced anomalous anticyclones over Eastern Europe, Northeast Asia, the Central-North Pacific and Northeast Canada, as well as weak anomalous cyclones in between (Fig. 4a). The response amplitudes of the anomaly centers are around 15~30 m, which pass the 90% confidence level. The corresponding low-level wave train in mid-high latitudes (Fig. 4b) indicates the nature of barotropic response. Besides the remarkable zonal wave train at upper level, there is a meridional wave train along the East Asian coast at low level with an anomalous cyclone over the western tropical Pacific and anomalous anticyclones over the Northeast Asia-North Pacific (denoted in Fig. 4b). This is consistent with the circulation leading to the East Asian precipitation anomalies in Fig. 2. The meridional wave train is somewhat similar to the Pacific-Japan (PJ) pattern in boreal summer (Nitta, 1987), but with a larger scale in the meridional direction.

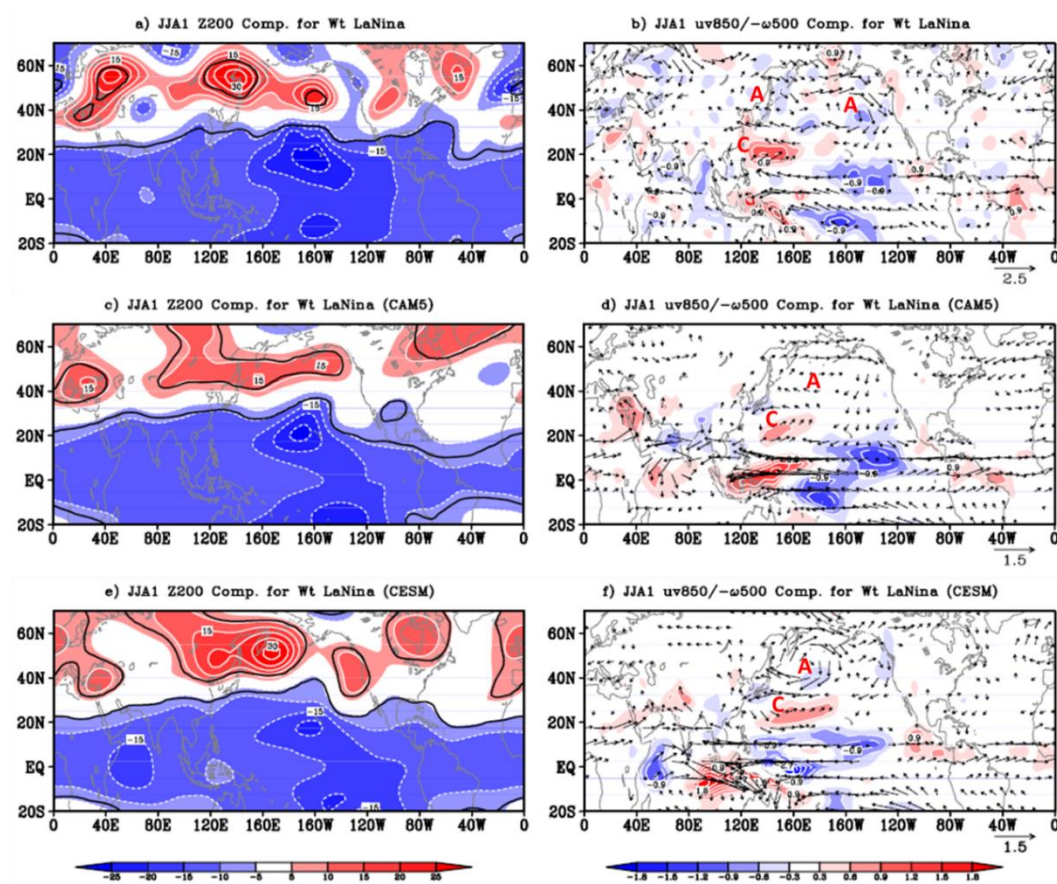


**Figure 4** Composite atmospheric anomalies in La Niña-decaying summer. From top to bottom are derived from the NCEP reanalysis data, the GOGA experiment of CAM5 and the Pacific

pacemaker experiment of CESM respectively. Left panels are 200-hPa geopotential height (shading,  $CI = 5 m$ ). The black contours denote the 90% confidence level. Right panels are 850-hPa wind (vector,  $m/s$ , omitted if less than one-tenth of the wind vector scalar) and 500-hPa vertical velocity omega with opposite sign ( $-\omega$ , shading,  $CI=0.3 \times 10^{-2} Pa/s$ , ascending in red and descending in blue). The red letters “C” and “A” mark cyclones and anticyclones respectively.

## b. Possible impact mechanism

To investigate physical mechanisms by which the intermediate SST anomaly in the tropical-North Pacific impacts the atmospheric circulation (as shown in Fig. 4a and b), we first examine the tropical precipitation anomalies in the following summer after La Niña peaks. As shown in Fig. 5a and b, the pronounced common feature of both precipitation and OLR is the undulated pattern along the tropical Oceans, with deficient rainfalls over the central tropical Pacific and Indian Ocean, and abundant rainfalls in the western equatorial Pacific and Atlantic. The last structures are elongated into the north subtropical Pacific and North Africa respectively. The ‘V’-shape negative precipitation anomalies over the central equatorial Pacific correspond well to the tropical part of the intermediate SST anomalies (Fig. 3c) and its associated vertical velocity change in the middle troposphere (Fig. 4b), which indicates the primary role of the intermediate SST anomalies on precipitation. Through the Walker circulation, the SST anomalies lead to positive precipitation anomalies over the [tropical Atlantic and over the western tropical Pacific](#), while negative precipitation anomalies over the tropical Indian Ocean.

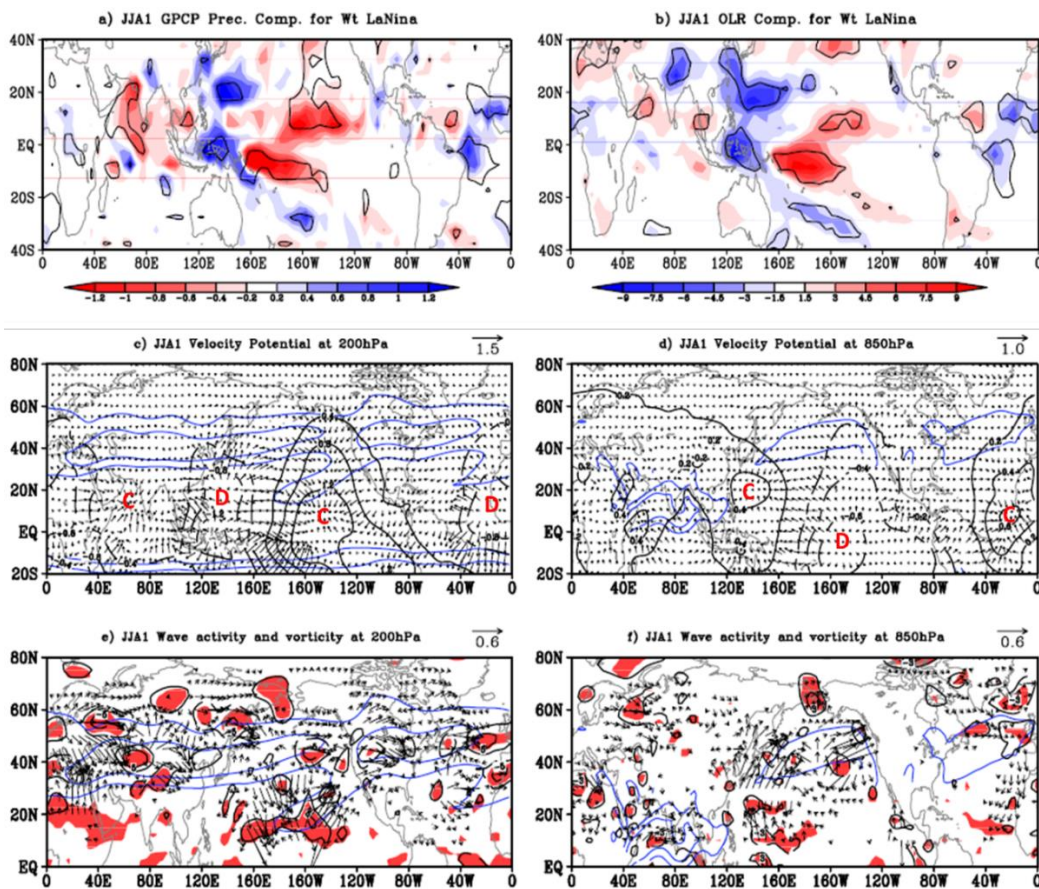


**Figure 5** Composite anomalies from NCAR-NCEP reanalysis data in La Niña-decaying summer. Upper panels are for precipitation ( $CI=0.2 mm/day$ ) (a) and OLR ( $CI=1.5 w/m^2$ )

(b) with black contours indicating the 90% confidence level. Middle panels are velocity potential (black contours, unit:  $10^6 m^2/s$ ) and divergence wind (vector, unit:  $m/s$ ) at 200-hPa (c) and 850-hPa (d), with red letters “C” and “D” denoting convergence and divergence. Bottom panels are wave activity flux (vector, unit:  $m^2/s^2$ , small values omitted if less than one-tenth of the vector scale) and vorticity (black contours, unit:  $10^6 s^{-1}$ ) at 200-hPa (e) and 850-hPa (f), with red shading indicating the 90% confidence level. In the middle and bottom panels, the blue contours denote the climatological westerly wind with speed of 10, 20  $m/s$  at 200-hPa and 5, 10  $m/s$  at 850-hPa.

We further investigate the heating - induced convergence and divergence in the atmosphere and the wave activities allowing atmospheric perturbations to propagate across the globe. As shown in Fig. 5c and d, cold SST anomalies in the eastern-central tropical Pacific cause local wind divergence at low level and convergence at upper level. Although the spatial extent of the perturbation is not very large, it is big enough for the perturbation to penetrate into the subtropical jet through the westerly trough over the eastern-central subtropical Pacific. Such as shown in Fig. 5e, the wave activity flux emanates from a positive vorticity over the northeast subtropical Pacific, which corresponds to the asymmetric Rossby wave response to SST anomalies, into the subtropical jet through the channel of the westerly trough (Wen et al., 2019). Due to the wave guide effect of the westerly jet, the perturbation - induced Rossby wave may propagate downstream along the jet, as indicated by the zonal eastward propagating energy flux (Fig. 5e).

Correspondingly, over the western tropical Pacific, wind converges at lower level and diverges at upper level, which results in abundant precipitation there. The divergence center in Fig. 5c is stretched into the far North Pacific, so that perturbations can directly enter into the subtropical jet and lead to the wave train response in mid-high latitudes (Wu et al., 2012). More importantly, the perturbation over the western tropical Pacific can excite the low-level meridional propagating Rossby wave train through the monsoon trough. As shown in Fig. 5f, the energy flux emits from the area of negative vorticity over the western tropical Pacific, which corresponds to the Rossby wave response to the intermediate SST anomalies in low level. It penetrates into a zone of positive vorticity over the western subtropical Pacific and continues to propagate into the North Pacific along the westerly jet. Conversely, the energy flux in upper level propagates southward from northeast Asia to the central subtropical Pacific. The structure of the energy propagation is consistent with that of the PJ pattern (Kosaka and Nakamura, 2010) which can be regarded as a dynamical mode of a particular mean state. Under the specific monsoonal circulation background over East Asia, the subtropical anticyclone near the surface and the upper-level subtropical jet constitutes a favorable configuration for the meridional wave (PJ pattern) to gain energy from the mean flow. Although the wave train along the East Asian coast in Fig. 4b is a bit different from the canonical PJ pattern, it can be strongly related to the enhanced convection activities over the Philippine Sea, originally initiated by the intermediate SST anomalies in the eastern-central tropical Pacific. Actually, the easterly and southwesterly wind anomalies, associated with the anomalous anticyclone over the western tropical Pacific (Fig. 4b), strengthen the convergence of the monsoon trough and lead to unusually heavy precipitation over the Philippine Sea (Fig. 5a) and to the northward propagating wave train. This pathway is quite similar to the route from the western tropical Pacific to North America in the persistent year of La Niña (Jong et al., 2020).

In addition to the above two pathways, there is possibly another route by which the intermediate SST anomalies impact the mid-latitude circulation. Similar to what in the western tropical Pacific, there is also a large wind perturbation in the tropical Atlantic. As shown in Fig. 5c and d, there is a competing divergence (convergence) in the upper (low) level over the tropical Atlantic – Northwest Africa, corresponding to the abnormal

precipitation there in Fig. 5a and b. Wind disturbances are just at the entrance of the south branch of the subtropical jet over the North Atlantic. They can easily enter into the subtropical jet and then trigger the downstream wave along the jet. This is clearly evidenced by the energy flux propagation over the eastern tropical Atlantic in Fig. 5e and f. In upper level, the energy flux propagates into the subtropical jet through the westerly trough extending toward the tropical Atlantic. However, in low level, the propagation is southward, opposite to the upper level. It is similar to the case of the energy propagation in the eastern-central subtropical Pacific through the westerly trough over the northeast subtropical Pacific. But there is a significant difference. Perturbations over the eastern-central tropical Pacific are directly induced by the intermediate SST anomalies, while those over the western tropical Pacific and the tropical Atlantic – Northwest Africa are results of indirect effects through the Walker circulation.

Although there is convergence over the tropical Indian Ocean in Fig. 5c, the perturbation is weak and mainly confined in the tropics. Therefore, the tropical Indian Ocean doesn't seem to exert its influence beyond the tropics (Wen et al., 2020). Overall, besides their effect on the tropical low-pressure belt through the Kelvin wave adjustment, the intermediate SST anomalies in the tropical-North Pacific might affect the mid-latitude circulation in three pathways. The first one is through the westerly trough over the eastern-central subtropical Pacific where heating-induced perturbations can easily penetrate into the subtropical jet, and generate wave train propagation along the jet. The second one is through the western Pacific monsoon trough where atmospheric perturbations can stimulate low-level meridional wave trains along the East Asian coast. And the third one is through the south branch of the North Atlantic subtropical jet that may convey wave propagation in it. These pathways are similar to those of the summer El Niño SST forcing onto the atmosphere in the developing summer (Wen et al., 2019, 2020), although the SST anomaly pattern and position seem very different from the summer El Niño SST anomalies. This may be due to the geographical advantage of the intermediate SST anomalies, especially the SST anomalies in the northeast subtropical Pacific, which is just under the westerly trough over the eastern-central subtropical Pacific.

## 5. Verification through numerical modelling

In this section, we use existing ocean-atmosphere coupled model simulations to check how observation-based results can be reproduced.

### a. GOGA experiment

We first examine the CAM5 GOGA experiment, in which any influence of other underlying surface forcings was excluded and only the effect of SST anomalies was considered. To similar SST forcing as shown in Fig. 3c, the model atmospheric response can well reproduce the observation results in Fig. 4a and b. As shown in Fig. 4c, the tropical atmosphere in upper level presents a low-pressure belt response with a pair of asymmetric Rossby waves across the eastern-central equatorial Pacific, which is consistent with the observation in Fig. 4a. The simulated wave train in mid-latitudes is relatively weak, but the anticyclonic centers are roughly collocated with the observations, especially for the anticyclone over northeast Asia. At low level, besides the similar tropical atmospheric response, the model can also reproduce the observed meridional wave train, although it is slight away from the East Asian coast (Fig. 4d). The consistent results between the model and the observation consolidate the role and effects of SST anomalies (as shown in Fig. 3c) on atmospheric circulation (Fig. 4a and b).

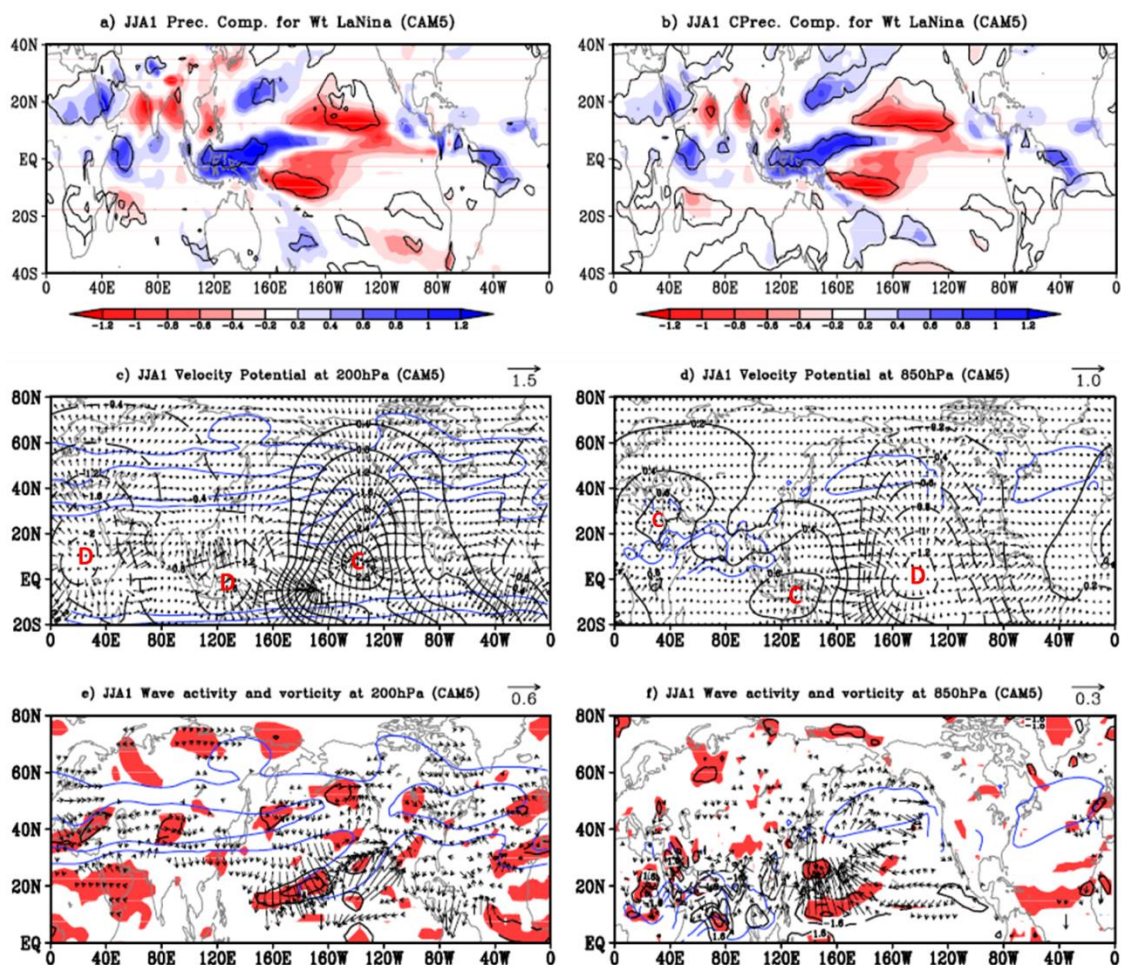


**Figure 6** Similar to Fig. 5, but for the Global Ocean Global Atmosphere (GOGA) experiment of the Community Atmosphere Model version 5 (CAM5). a) and b) are total precipitation and convective precipitation anomalies ( $CI=0.2 \text{ mm/day}$ ). c) and d) are velocity potential (black contours, unit:  $10^6 \text{ m}^2/\text{s}$ ) and divergence wind (vector, unit:  $\text{m/s}$ ) at 200-hPa and 850-hPa. e) and f) are wave activity flux (vector, unit:  $\text{m}^2/\text{s}^2$ , small values omitted if less than one-tenth of the vector scale) and vorticity (black contours, unit:  $10^6 \text{ s}^{-1}$ ) at 200-hPa and 850-hPa. The red letters “C” and “D” mark the convergence and divergence wind. The blue contours denote the climatological westerly wind with speed of 10, 20  $\text{m/s}$  at 200-hPa and 5, 10  $\text{m/s}$  at 850-hPa. Note that the scale of vectors in Panel f is half of what used in Panel e.

The model can also simulate the main pathways by which the SST anomaly impacts the atmospheric circulation. As shown in Fig. 6a and b, the induced dryness over the central tropical Pacific basically reproduces the observation results, although the pattern is split into two parts with the northern part slightly away from the equator. The surrounding wet conditions are mainly confined to the equatorial Pacific, which are somewhat different from the observations. The corresponding wind shows a dominant convergence at upper level (Fig. 6c) covering the whole eastern-central tropical and North Pacific, with opposite conditions at low level. The upper-level atmospheric circulation shows a large-scale divergence in North Africa and the tropical Indian Ocean, with a subordinate center in the western tropical Pacific. As a result, there are prominent positive precipitation anomalies over Northeast Africa and the western tropical Pacific. These characteristics are slightly different from the observations, showing several competing divergences (Fig. 5c) and precipitations (Fig. 5a) over the western tropical Pacific and the tropical Atlantic – Northwest Africa. Corresponding to the wind

perturbation, it is clear that the energy flux over the eastern-central tropical Pacific is effectively transmitted into the subtropical jet through the westerly trough and then propagates downstream along the jet (Fig. 6e). Despite the limited amplitude of the wind perturbation over the western tropical Pacific, there is still the northward propagation wave through the monsoon trough, as indicated by the propagation of energy flux along the coast of East Asia (Fig. 6f). The two pathways are consistent with those observed. However, relative to the observation, the third pathway of the model is slightly shifted to the east of North Africa. As shown in Fig. 6e, the energy flux propagates from North Africa to mid-high latitudes, which corresponds well to the wave train over Northern Eurasia (Fig. 4c). That causes perturbations over Northeast Africa, which are located on the west side of the South Asian High, and can be transmitted by the southerly wind into extra-tropics and then stimulate the northeastward propagating wave in mid-high latitudes (Wang et al., 2005). This is consistent with the findings of Wen et al. (2020) in terms of different types of El Niño influence on the atmosphere. Overall, the model can reproduce the main effect of intermediate SST anomalies on the atmospheric circulation in observation, which enhances our confidence for the proposed physical mechanism.

### **b. Pacific pacemaker experiment**

Using the CESM Pacific pacemaker experiment, we demonstrate that winter-peaked La Niña can indeed trigger intermediate SST anomalies in subsequent seasons (spring and summer), as identified in the observation. As shown in Fig. 3d, e and f, La Niña can initiate SST anomalies along the west coast of North America in winter. They are amplified in the following spring (Fig. 3e) and remain persistent in the following summer (Fig. 3f), which resembles the ‘Z’ shape SST anomalies in the tropical - northern Pacific in Fig. 3c (observation). However, unlike the observation, the model shows a strong relation of winter La Niña with the basin-scale cold SST in the tropical Indian Ocean, where the SST anomalies generated in winter can be sustained into the following summer. Despite the discrepancies for the simulated SST anomalies in the following summer, CESM can still reproduce the main characteristics of the atmospheric responses in observation. As shown in Fig. 4e, the atmospheric response at upper level is also a low - pressure belt in the tropics with a pair of asymmetric cyclones over the eastern - central tropical Pacific and a salient wave train in mid-latitudes. At low level, Figure 4f also shows a meridional wave train slightly away from the East Asian coast. Compared with the GOGA experiment, there are some differences for the pacemaker results, such as the largely amplified anticyclone over the zone of northeast Asia - Northwest Pacific and enhanced circulation anomalies along the East Asian coast. That might be the joint effect of the SST anomaly forcing over the tropical Indian Ocean. Furthermore, we also examine how the SST anomalies in Fig. 3f exert their influence on the circulation. Despite the interference of the tropical Indian Ocean, the first two pathways of the observations for SST anomalies to affect the atmospheric circulation are clearly simulated (as shown in supplementary figure 4). This further confirms the ‘bridge’ role of the SST anomalies in the tropical-North Pacific in relaying the winter-peaked La Niña effect into the following summer.

In addition, we also examined the model - simulated precipitation and associated key circulation patterns over East Asia in the following summer after La Niña peaks in boreal winter. As shown in the supplementary Fig. 3, the model can capture the main features of the circulation in Fig. 2, such as the anomalous anticyclone over Northeast Asia and the anomalous cyclone over the western subtropical Pacific. But, the two key circulations are slightly shifted to the southeast. This results in a southeastward displacement of the entire rainband in the model, relative to the observation in Fig. 1b. Overall, the model results can roughly demonstrate the delayed effect of La Niña on the following summer East Asian climate through the intermediate SST anomalies identified in Fig. 3.

## 6. Summary and discussion

This paper aims to investigate impacts of boreal winter-peaked La Niña on the following summer East Asian precipitation and to study how the intermediate SST anomalies can sustain the delayed effect of La Niña on the atmospheric general circulation. Our result indicates that, in the decaying summer of La Niña, precipitation shows anomalous dryness in North and South China, but anomalous wetness in east coasts of central China. Such a precipitation pattern is attributed to two key atmospheric circulation structures: the anomalous cyclone over the western tropical Pacific and the anomalous anticyclone over Northeast Asia. It is also shown that winter - peaked La Niña affects the East Asian climate in the following summer mainly through intermediate SST anomalies --- a 'Z' shape cold SST over the tropical - North Pacific (as shown by the schematic in Fig. 7). It should be noted here that the intermediate SST anomalies actually include the residual SST anomalies of La Niña in the central equatorial Pacific, which can exert direct effect of La Niña's persistence in summer (DiNezio and Deser, 2014; Okumura et al., 2017; Song et al., 2022; Anderson et al., 2023).

To the intermediate SST anomaly forcing, the atmospheric circulation shows a low - pressure belt response in the tropics due to equatorial Kelvin wave adjustment. In mid-latitudes, the atmospheric response presents a zonal wave train in upper level and a meridional propagating wave in low level. Three pathways were suggested for the intermediate SST anomalies to affect the mid-latitude atmospheric circulation (as illustrated by the schematic in Fig. 7). One refers to the fact that the SST anomaly - induced perturbations are transmitted into the subtropical jet through the westerly trough over the northeast subtropical Pacific, which in turn stimulates the wave train propagation along the jet. Another is that the SST anomaly - associated perturbations excite the northward propagating wave along the East Asian coast through the monsoon trough over the western Pacific. And the last one is that the SST anomaly - associated perturbations over the tropical Atlantic - Northwest Africa can trigger the downstream propagating wave through the south branch of the North Atlantic subtropical jet.

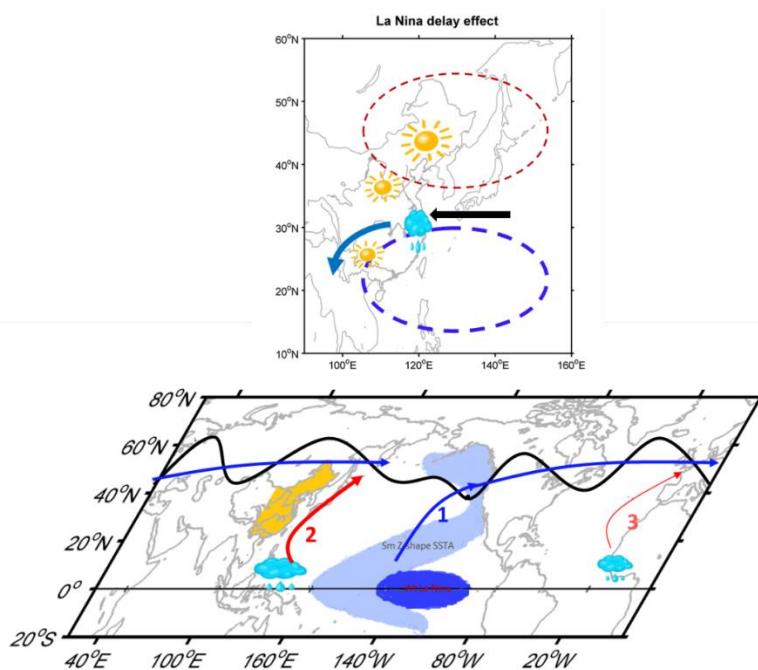


**Figure 7** Schematic showing winter-peaked La Niña impact on the following summer East Asian precipitation through intermediate SST anomalies in the tropical-North Pacific.

Precipitation anomalies, together with an anomalous cyclone over the western subtropical Pacific (blue dashed oval) and an anomalous anticyclone over Northeast Asia (dark red dashed circle), are shown in the upper panel. These precipitation and circulation anomalies are fundamentally caused by the winter La Niña - associated intermediate SST anomalies showing a Z shape in the following summer in the tropical-North Pacific (light blue shadings), as indicated in the bottom panel. The intermediate SST anomalies exert influence on atmospheric circulation following three pathways. One is near the westerly trough over the northeast subtropical Pacific (as indicated by the blue curve). Another is through the monsoon trough over the western Pacific (as indicated by the red curve). The last one is connected to the south branch of the North Atlantic subtropical jet (as indicated by the light red curve).

To confirm the role of the intermediate SST anomalies and their operating mechanism on atmospheric circulation, we further analyzed the existing GOGA and Pacific-pacemaker experiments conducted with CAM and CESM. The model well reproduced the atmospheric circulation anomalies and the first two affecting pathways over the northeast subtropical Pacific and the western Pacific. It is also confirmed that the winter La Niña SST anomalies in the eastern-central tropical Pacific can indeed induce the 'Z' shape cold SST anomaly over the tropical - northern Pacific. However, the model generated too strong large-scale wind convergence / divergence, and the third pathway in the observation looks much drifted to Northeast Africa. The relationship between ENSO and the SST anomalies in the tropical Indian Ocean is also slightly stronger in the model.

In this study, we focused on the recent period of 1979~2020, which is posterior to the climate shift that occurred in East Asia in 1976/1977 (Ding et al., 2007). Our choice was intended to avoid possible interference from interdecadal variability. According to Yuan et al. (2014), the influence of La Niña on simultaneous winter precipitation in southern China presented a clear decadal change around 1980. Therefore, the robustness of our findings (including relevant mechanisms) deserves a short discussion in terms of interdecadal variation of the regional climate. Actually, we did prolong our investigation period and extended it back to 1958. Three strong La Niña events were identified from 1958 to 1978. There are some variations in local precipitation, such as in South China (as shown in SFig. 1b), which is certainly the manifestation of the interdecadal variation. Despite a few subtle differences, main large-scale characteristics that we present here remain unchanged, such as the widespread anomalous dryness in North China and the anomalous wetness along the east coast of China (properties shown in SFig. 1b and 2b). It should also be noted that other features in terms of atmospheric circulation, intermediate SST anomalies and relevant physical mechanisms, have no significant changes neither (Figures not shown). This illustrates the stability and representativeness of our conclusions.

From our analysis, we can see that the intermediate SST anomalies that relay La Niña's delay effect into the following summer are quite different from El Niño (Xie et al., 2016; Li et al., 2017). This can be considered as a manifestation of the asymmetry between the two phases of the ENSO cycle, largely due to nonlinear processes of both ocean and atmosphere (Hoerling et al., 1997; Ohba and Ueda, 2009; Chen et al., 2016; Okumura, 2019). However, when choosing La Niña index, we find that the circulation response (especially for precipitation anomalies over East Asia) is more sensitive to SST anomaly in the central Pacific than that in the eastern Pacific. This may also be related to nonlinear processes in the atmosphere, in particular, to the threshold issue of atmospheric convection. It implies that La Niña might also need to be typed to study its climate effects in the decaying summer, as is usually the case for El Niño (WLH22). In addition, we can observe many continuous La Niña cases in the past. How the intermediate SST anomalies in the tropical - North Pacific contribute to the continuity of La Niña through its induced easterly anomalies in the far western tropical Pacific, would be specifically discussed in a separate paper.

Some other issues also need to be addressed in the future. For example, our present study can't distinguish the propagation modes or regimes within the subtropical jet for the three pathways connecting tropical perturbations to mid and high latitudes. Further investigation is needed to accurately determine the propagation modes through the use of simplified dynamic models, such as the stationary wave model (Ting and Hoerling, 1993) or the linear baroclinic model (Watanabe and Kimoto, 2000).

### Acknowledgement

This work is supported by the Natural Science Foundation of China (NSFC41475089) and National Key R&D Program of China (2020YFA0608901). Laurent Li acknowledges French GENCI for allocation of computing resources. We are grateful for the Editor and three anonymous Reviewers for their constructive comments.

### Data Availability Statement

The model simulations presented in Section 5 are conducted by the NCAR CESM Climate Variability & Change Working Group. The simulation data is openly available at the website ([https://www.cesm.ucar.edu/working\\_groups/CVC](https://www.cesm.ucar.edu/working_groups/CVC)).

### References

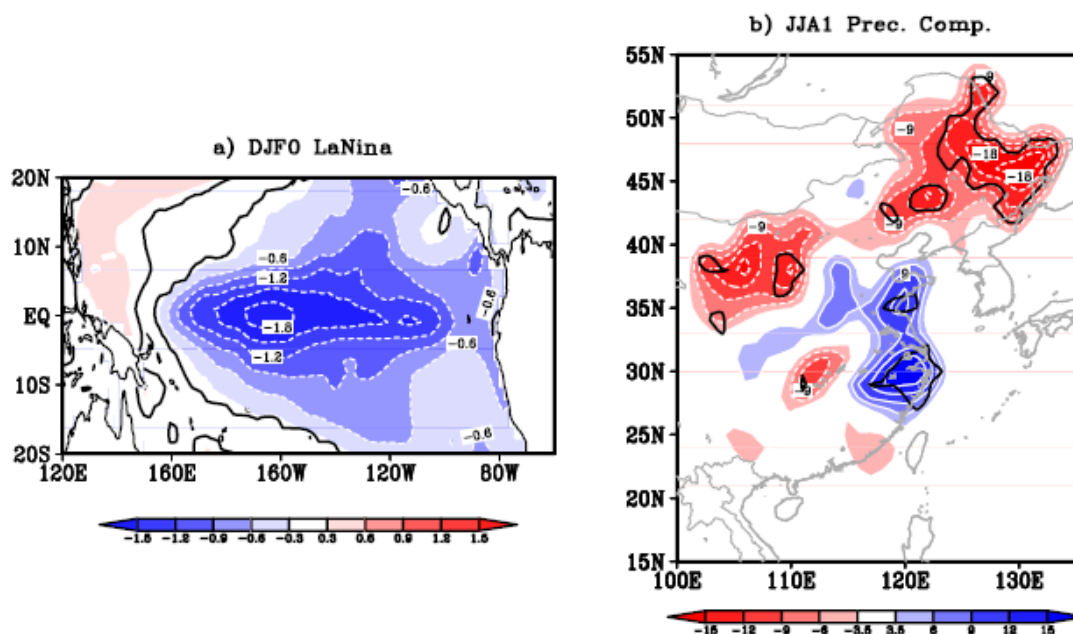
- An, S.-I., and F.-F. Jin, 2004: Nonlinearity and asymmetry of ENSO. *J. Climate*, **17**, 2399-2412, [https://doi.org/10.1175/1520-0442\(2004\)017<2399:NAAOE>2.0.CO;2](https://doi.org/10.1175/1520-0442(2004)017<2399:NAAOE>2.0.CO;2).
- Anderson, W., B. I. Cook, K. Slinski, K. Schwarzwald, A. McNally, and C. Funk, 2023: Multiyear La Niña events and multiseason drought in the Horn of Africa. *J. Hydrometeorology*, **24**, 119-131, <https://doi.org/10.1175/JHM-D-22-0043.1>.
- Ashok, K., S. K. Behera, S. A. Rao, and Coauthors, 2007: El Niño Modoki and its possible teleconnection. *J. Geophys. Res.*, **112**, C11007, <https://doi.org/10.1029/2006JC003798>.
- Ashok K , Shamal M , Sahai A K , et al., 2017, Nonlinearities in the Evolutional Distinctions Between El Niño and La Niña Types[J]. *Journal of Geophysical Research: Oceans*, **122**, 9649-9662, <https://doi.org/10.1002/2017JC013129>.
- Chang, C. P., Y. Zhang, T. Li, 2000: Interannual and Interdecadal Variations of the East Asian Summer Monsoon and Tropical Pacific SSTs. Part II: Meridional Structure of the Monsoon[J]. *Journal of Climate*, **13**(24), 4326-4340, [https://doi.org/10.1175/1520-0442\(2000\)013<4326:IAIVOT>2.0.CO;2](https://doi.org/10.1175/1520-0442(2000)013<4326:IAIVOT>2.0.CO;2).
- Chen, M., Li, T., Shen, X., and Wu, B., 2016: Relative Roles of Dynamic and Thermodynamic Processes in Causing Evolution Asymmetry between El Niño and La Niña, *Journal of Climate*, **29**, 2201-2220, <https://doi.org/10.1175/JCLI-D-15-0547.1>.
- Chelton, D. B. and R. E. Davis, 1982: Monthly mean sea-level variability along the west coast of North America. *J. Phys. Oceanogr.*, **12**, 757-783, [https://doi.org/10.1175/1520-0485\(1982\)012<0757:MMSLVA>2.0.CO;2](https://doi.org/10.1175/1520-0485(1982)012<0757:MMSLVA>2.0.CO;2).
- Choi, K.-Y., G. A. Vecchi, and A. T. Wittenberg, 2013: ENSO transition, duration, and amplitude asymmetries: Role of the nonlinear wind stress coupling in a conceptual model. *J. Climate*, **26**, 9462-9476, <https://doi.org/10.1175/JCLI-D-13-00045.1>.
- DiNezio, P. N., and C. Deser, 2014: Nonlinear controls on the persistence of La Niña. *J. Climate*, **27**, 7335-7355, <https://doi.org/10.1175/JCLI-D-14-00033.1>.
- Ding Y, Z. Wang, and Y. Sun, 2007: Interdecadal variation of the summer precipitation in East China and its association with decreasing Asian monsoon. Part I: observed evidences. *Int. J. Climatol.*, **28**, 1139-1161, <https://doi.org/10.1002/joc.1615>.
- Dommenget, D., T. Bayr, and C. Frauen, 2013: Analysis of the non-linearity in the pattern and time evolution of El Niño Southern Oscillation. *Climate Dyn.*, **40**, 2825-2847, <https://doi.org/10.1007/s00382-012-1475-0>.
- Eisenman, I., L. S. Yu, and E. Tziperman, 2005: Westerly wind bursts: ENSO's tail rather than the

- dog? *J. Climate*, **18**, 5224-5238, <https://doi.org/10.1175/JCLI3588.1>.
- Gadgil, S., P. V. Joseph, and N. V. Joshi, 1984: Ocean-Atmosphere coupling over monsoon regions, *Nature*, **312**, 141– 143, <https://doi.org/10.1038/312141a0>.
- Gill, A. E., 1980: Some simple solutions for heat-induced tropical circulation, *Q. J.R. Meteorol. Soc.*, **106**, 447-462, <https://doi.org/10.1002/qj.49710644905>.
- Hoskins, B. J., and D. J. Karoly, 1981: The steady linear response of a spherical atmosphere to thermal and orographic forcing. *J. Atmos. Sci.*, **38**, 1179-1196, [https://doi.org/10.1175/1520-0469\(1981\)038<1179:TSLROA>2.0.CO;2](https://doi.org/10.1175/1520-0469(1981)038<1179:TSLROA>2.0.CO;2).
- Hoerling, M. P., A. Kumar, and M. Zhong, 1997: El Niño, La Niña, and the nonlinearity of their teleconnections. *J. Climate*, **10**, 1769-1786, [https://doi.org/10.1175/1520-0442\(1997\)010<1769:ENOLNA>2.0.CO;2](https://doi.org/10.1175/1520-0442(1997)010<1769:ENOLNA>2.0.CO;2).
- Jong, B.-T., M. Ting, R. Seager, and W. B. Anderson, 2020: ENSO teleconnections and impacts on U.S. summertime temperature during a multiyear La Niña life cycle. *J. Climate*, **33**, 6009-6024, <https://doi.org/10.1175/JCLI-D-19-0701.1>.
- Kalnay, E., M. Kanamitsu, R. Kistler, W. Collins, D. Deaven, L. Gandin, M. Iredell, S. Saha, G. White, J. Woollen, Y. Zhu, M. Chelliah, W. Ebisuzaki, W. Higgins, J. Janowiak, K. C. Mo, C. Ropelewski, J. Wang, A. Leetmaa, R. Reynolds, Roy Jenne, and Dennis Joseph, 1996: The NCEP/NCAR 40-year reanalysis project. *Bull Amer Meteorol Soc*, **77**:437-471, [https://doi.org/10.1175/1520-0477\(1996\)077<0437:TNYRP>2.0.CO;2](https://doi.org/10.1175/1520-0477(1996)077<0437:TNYRP>2.0.CO;2).
- Kao, H. Y., and J. Y. Yu, 2009: Contrasting eastern-Pacific and central-Pacific types of ENSO, *J. Climate*, **22**, 615-632, <https://doi.org/10.1175/2008JCLI2309.1>.
- Kang, I.-S., and J.-S. Kug, 2002: El Niño and La Niña sea surface temperature anomalies: Asymmetry characteristics associated with their wind stress anomalies. *J. Geophys. Res.*, **107**(D19), 4372, <https://doi.org/10.1029/2001JD000393>.
- Kim, D., S. - K. Lee and H. Lopez, 2020: Madden - Julian Oscillation - induced suppression of northeast Pacific convection increases U.S. tornadogenesis. *Journal of Climate*, **33**(11), 4927-4939, <https://doi.org/10.1175/JCLI-D-19-0992.1>.
- Kosaka, Y., and H. Nakamura, 2010: Mechanisms of meridional teleconnection observed between a summer monsoon system and a subtropical anticyclone. Part I: The Pacific-Japan pattern, *J. Clim.*, **23**:5085-5108, <https://doi.org/10.1175/2010JCLI3413.1>.
- Kug, J. S., F. F. Jin, and S. L. An, 2009: Two types of El Niño events: cold tongue El Niño and warm pool El Niño, *J. Climate*, **22**, 1499-1515, <https://doi.org/10.1175/2008JCLI2624.1>.
- Kug, J. S., and Y. G. Ham, 2011: Are there two types of La Niña? 2011, *Geophysical Research Letters*, **38**, L16704, <https://doi.org/10.1029/2011gl048237>.
- Li, T., B. Wang, B. Wu, T. Zhou, C.P. Chang, and R. Zhang, 2017: Theories on formation of an anomalous anticyclone in western North Pacific during El Niño: A review. *Journal of Meteorological Research*, **31**(6), pp.987-1006, <https://doi.org/10.1007/s13351-017-7147-6>.
- Li, Z. X. and S. Conil, 2003: Transient Response of an Atmospheric GCM to North Atlantic SST Anomalies, *J. Climate*, **16**, 3993-3998, [https://doi.org/10.1175/1520-0442\(2003\)016<3993:TROAAG>2.0.CO;2](https://doi.org/10.1175/1520-0442(2003)016<3993:TROAAG>2.0.CO;2).
- McPhaden, M. J., and X. Zhang, 2009: Asymmetry in zonal phase propagation of ENSO sea surface temperature anomalies. *Geophys. Res. Lett.*, **36**, L13703, <https://doi.org/10.1029/2009GL038774>.
- Mantua, N. J., S. R. Hare, Y. Zhang, J. M. Wallace, and R. C. Francis, 1997: A Pacific interdecadal climate oscillation with impacts on salmon production, *Bull. Amer. Meteor. Soc.*, **78**, 1069–1079, [https://doi.org/10.1175/1520-0477\(1997\)078<1069:APICOW>2.0.CO;2](https://doi.org/10.1175/1520-0477(1997)078<1069:APICOW>2.0.CO;2).
- Nitta, T., 1987: Convective activities in the Tropical Western Pacific and their impact on the Northern Hemisphere summer circulation, *J Meteor Soc Japan*, **65**, 373-390, [https://doi.org/10.2151/jmsj1965.65.3\\_373](https://doi.org/10.2151/jmsj1965.65.3_373).
- Ohba, M., and H. Ueda, 2009: Role of nonlinear atmospheric response to SST on the asymmetric transition process of ENSO. *J. Climate*, **22**, 177-192, <https://doi.org/10.1175/2008JCLI2334.1>.
- Okumura, Y. M., 2019: ENSO diversity from an atmospheric perspective. *Curr. Climate Change Rep.*, **5**, 245-257, <https://doi.org/10.1007/s40641-019-00138-7>.

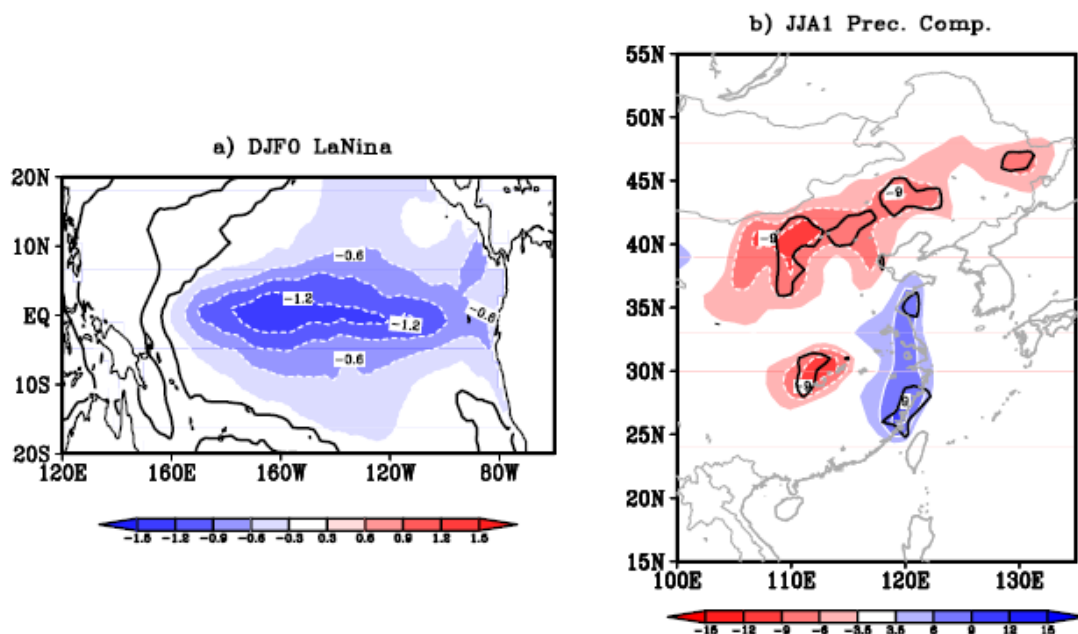
- Okumura, Y. M., and C. Deser, 2010: Asymmetry in the duration of El Niño and La Niña. *J. Climate*, **23**, 5826-5843, <https://doi.org/10.1175/2010JCLI3592.1>.
- Okumura, Y. M., P. DiNezio, P., and C. Deser, 2017: Evolving impacts of multiyear La Niña events on atmospheric circulation and U.S. drought. *Geophysical Research Letters*, **44**, 11,614–11,623. <https://doi.org/10.1002/2017GL075034>
- Peng, S., and J.S. Whitaker, 1999: Mechanisms determining the atmospheric response to midlatitude SST anomalies. *J. Clim.*, **12**, 1393-1408, [https://doi.org/10.1175/1520-0442\(1999\)012<1393:MDTART>2.0.CO;2](https://doi.org/10.1175/1520-0442(1999)012<1393:MDTART>2.0.CO;2).
- Rasmusson, E. M., and T. H. Carpenter, 1982: Variations in tropical sea surface temperature and surface wind fields associated with the Southern Oscillation/El Niño. *Mon. Wea. Rev.*, **110**, 354–384, [https://doi.org/10.1175/1520-0493\(1983\)111<1338:R>2.0.CO;2](https://doi.org/10.1175/1520-0493(1983)111<1338:R>2.0.CO;2).
- Ropelewski, C.F., and M.S. Halpert, 1987: Global and regional scale precipitation patterns associated with the El Niño/Southern Oscillation, *Mon. Weather Rev.*, **115**, 1606-1626, [https://doi.org/10.1175/1520-0493\(1987\)115.0.CO;2](https://doi.org/10.1175/1520-0493(1987)115.0.CO;2).
- Rong, X. Y., R. H. Zhang, and T. Li, 2010: Impacts of Atlantic sea surface temperature anomalies on Indo-East Asian summer monsoon-ENSO relationship. *Chinese Science Bulletin*, **55**, 2458–2468, <https://doi.org/10.1007/s11434-010-3098-3>.
- Rong, X., R. Zhang, T. Li, and J. Su, 2011: Upscale feedback of highfrequency winds to ENSO. *Quart. J. Roy. Meteor. Soc.*, **137**, 894-907, <https://doi.org/10.1002/qj.804>.
- Schwing, F. B., T. Murphree, L. deWitt, and P. M. Green, 2002: The evolution of oceanic and atmospheric anomalies in the northeast Pacific during the El Niño and La Niña events of 1995–2001, *Prog. Oceanogr.*, **54**, 459–491, [https://doi.org/10.1016/S0079-6611\(02\)00064-2](https://doi.org/10.1016/S0079-6611(02)00064-2).
- Shinoda T., H. E. Hurlburt, E. J. Metzger, 2011: Anomalous tropical ocean circulation associated with La Niña Modoki, *Journal of Geophysical Research*, **116**, C12001, <https://doi.org/10.1029/2011JC007304>.
- Song X, Zhang R, Rong X, 2022: Dynamic causes of ENSO decay and its asymmetry. *J. Climate*, **35**:445–462. <https://doi.org/10.1175/JCLI-D-21-0138.1>
- Su J. , R. Zhang, T. Li, X. Rong, et al., 2010: Causes of the El Niño and La Niña Amplitude Asymmetry in the Equatorial Eastern Pacific, *Journal of Climate*, **23**, 605-617, <https://doi.org/10.1175/2009JCLI2894.1>.
- Takaya K, H. Nakamura, 2001: A formulation of a phase-independent wave-activity flux for stationary and migratory quasigeostrophic eddies on a zonally varying basic flow, *J Atmos Sci*, **58**, 608-627, [https://doi.org/10.1175/1520-0469\(2001\)058<0608:AFOAPI>2.0.CO;2](https://doi.org/10.1175/1520-0469(2001)058<0608:AFOAPI>2.0.CO;2).
- Ting, M., and M. P. Hoerling, 1993: Dynamics of stationary wave anomalies during the 1986/87 El Niño. *Climate Dyn.*, **9**, 147–164, <https://doi.org/10.1007/BF00209751>.
- Vimont D J , J M Wallace, D S Battisti, 2002: The Seasonal Footprinting Mechanism in the Pacific: Implications for ENSO, *J. Climate*, **16**, 2668-2675, [https://doi.org/10.1175/1520-0442\(2003\)016<2668:TSMIT>2.0.CO;2](https://doi.org/10.1175/1520-0442(2003)016<2668:TSMIT>2.0.CO;2).
- Wang, B., and Q. Zhang, 2002: Pacific-East Asian Teleconnection. Part II : How the Philippine Sea Anomalous Anticyclone is Established during El Niño Development, *J. Climate*, **15**, 3252-3265, [https://doi.org/10.1175/1520-0442\(2002\)015<3252:PEATPI>2.0.CO;2](https://doi.org/10.1175/1520-0442(2002)015<3252:PEATPI>2.0.CO;2).
- Wang, B, R. Wu, and T. Li, 2003: Atmosphere–warm Ocean interaction and its impacts on Asian-Australian monsoonvariation. *Journal of Climate*, **16**, 1195–1211, [https://doi.org/10.1175/1520-0442\(2003\)16<1195:AOIAll>2.0.CO;2](https://doi.org/10.1175/1520-0442(2003)16<1195:AOIAll>2.0.CO;2).
- Wang Z, C. Chang, B. Wang, et al., 2005: Teleconnections from tropics to Northern extratropics through a southerly conveyor, *J Clim*, **62**:4057-4070, <https://doi.org/10.1175/JAS3600.1>
- Watanabe, M., & M. Kimoto, 2000: Atmosphere-ocean thermal coupling in the North Atlantic: A positive feedback. *Quarterly Journal of the Royal Meteorological Society*, **126**(570), 3343 – 3369. <https://doi.org/10.1002/qj.49712657017>.
- Wen, N., Z. Liu, and L. Li, 2019: Direct ENSO Impact on East Asian Summer Precipitation in the Developing Summer, *Clim. Dyn.*, **52**, 6799-6815, <https://doi.org/10.1007/s00382-018-4545-0>.

- Wen, N., L. Li, and J. Luo, 2020: Direct impacts of different types of El Niño in developing summer on East Asian precipitation, *Clim. Dyn.*, **55**, 1087-1104, <https://doi.org/10.1007/s00382-020-05315-1>.
- Wen, N. and Y. Hao, 2021: Contrasting El Niño impacts on East Asian summer monsoon precipitation between its developing and decaying stages, *International Journal Of Climatology*, **41**, 2375-2382, <https://doi.org/10.1002/joc.6964>.
- Wen, N., L. Li, and Y. Hao, 2022: Response of East Asian Summer Precipitation to Intermediate SST Anomalies while El Niño Decays and Dependence on Type of Events, *Journal of Climate*, **35**, 3845-3860, <https://doi.org/10.1175/JCLI-D-21-0335.1>
- Wu, B., T. Zhou, and T. Li, 2009: Seasonally evolving dominant interannual variability modes of East Asian climate. *Journal of Climate*, **22**, 2992-3005, <https://doi.org/10.1175/2008JCLI2710.1>.
- Wu, B., T. Li, and T. Zhou, 2010a: Asymmetry of atmospheric circulation anomalies over the Western North Pacific between El Niño and La Niña. *J. Climate*, **23**, 4807-4822, <https://doi.org/10.1175/2010JCLI3222.1>.
- Wu, Z. W., J.P. Li, ZH. Jiang, et al, 2012: Possible effects of the North Atlantic Oscillation on the strengthening relationship between the East Asian Summer monsoon and ENSO. *Int. J. Climatol.*, **32**, 794-800, <https://doi.org/10.1002/joc.2309>.
- Xie, S., K. Hu, J. Hafner, H. Tokinaga, Y. Du, G. Huang, and Sampe T., 2009: Indian Ocean capacitor effect on Indo-western Pacific climate during the summer following El Niño, *J. Climate*, **22**, 730 – 747, <https://doi.org/10.1175/2008JCLI2544.1>.
- Xie, S. P., K. Yu, Y. Du, K. Hu, J. S. Chowdary, G. Huang, 2016: Indo-western Pacific ocean capacitor and coherent climate anomalies in post-ENSO summer: a review. *Adv. Atmos. Sci.* **33**, 411–432, <https://doi.org/10.1175/2008JCLI2544.1>.
- Yang, J., Q. Liu, S-P, Xie, Z. Liu, L. Wu, 2007: Impact of the Indian Ocean SST basin mode on the Asian summer monsoon. *Geophys. Res. Lett.*, **34**, L02708, <https://doi.org/10.1029/2006GL028571>.
- Yuan, Y., and H. Yan, 2013: Different types of La Nia events and different responses of the tropical atmosphere[J], *Chinese Science Bulletin*, **58**, 406-415, <https://doi.org/10.1007/s11434-012-5423-5>.
- Yuan, Y., C. Li, S. Yang, 2014, Decadal anomalies of winter precipitation over southern China in association with El Niño and La Niña, *Acta Meteorological Sinica*, **72**, 237-255, <https://doi.org/10.11676/qxxb2014.014>.
- Zhang, R. H., A. Sumi, and M. Kimoto, 1999: A Diagnostic Study of the Impact of El Niño on the Precipitation in China, *Advances in Atmospheric Sciences*, **16**, 229-241, <https://doi.org/10.1007/BF02973084>.
- Zhou, T., Wu B., and D. Lu, 2014: Advances in research of ENSO changes and the associated impacts on Asian-Pacific climate[J]. *Asia-Pacific Journal of Atmospheric Sciences*, **50**, 405-422, <https://doi.org/10.1007/s13143-014-0043-4>.

## Supplementary Materials:



**SFigure 1** Same as Figure 1, the La Nina cases are selected based on the same criterion. But the period covers from 1958 to 2020, where 11 events are selected (1970/1971, 1973/1974, 1975/1976, 1988/1989, 1998/1999, 1999/2000, 2000/2001, 2007/2008, 2010/2011, 2011/2012 and 2020/2021).



**SFigure 2** Same as Figure 1, but the La Nina cases are selected according to the criteria of the Climate Prediction Center (CPC, [https://origin.cpc.ncep.noaa.gov/products/analysis\\_monitoring/ensostuff/ONI\\_v5.php](https://origin.cpc.ncep.noaa.gov/products/analysis_monitoring/ensostuff/ONI_v5.php)). During the period from 1958 to 2021, a total of 22 events are selected (1964/1965, 1967/1968,

1970/1971, 1971/1972, 1973/1974, 1974/1975, 1975/1976, 1983/1984, 1984/1985, 1988/1989, 1995/1996, 1998/1999, 1999/2000, 2000/2001, 2005/2006, 2007/2008, 2008/2009, 2010/2011, 2011/2012, 2016/2017 and 2017/2018, 2020/2021).

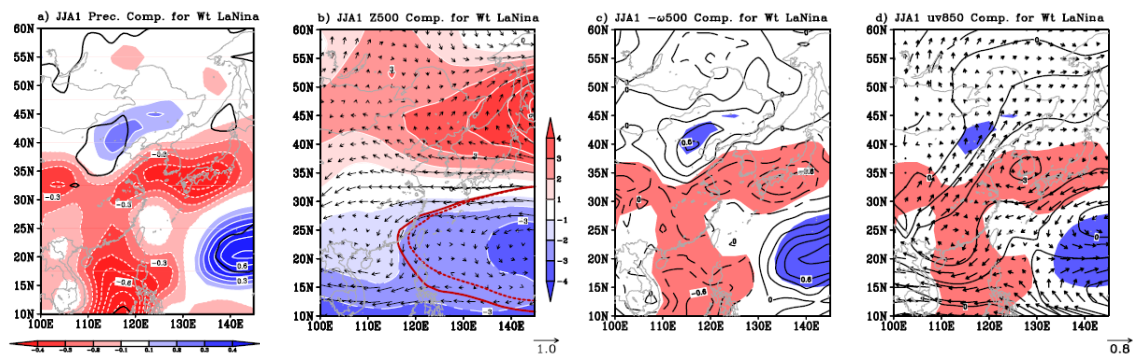


**Figure 3** Similar to Fig. 2 -- the regional precipitation and circulation anomalies over East Asia in La Niña-decaying summer, but for GOGA experiment of CAM5. a) precipitation anomalies with blue (red) shading indicating wetness (dryness) ( $CI=0.1 \text{ mm/day}$ ). Black contours indicate the 90% confidence level. b) 500-hPa geopotential height (shaded,  $CI=1 \text{ m}$ ) and wind (vector, unit:  $\text{m/s}$ ). The thick red dashed (solid) line denotes the composite (climatological) 5860 m geopotential height, indicating the position of the Western Pacific Subtropical high. c) 500-hPa vertical velocity ( $-\omega$ ) anomalies (black contours, unit:  $10^6 \text{ m}^2/\text{s}$ ). d) 850-hPa geopotential height (black contours,  $CI=1 \text{ m}$ ) and 850-hPa wind (vector, unit:  $\text{m/s}$ ). The shadings in the c and d represent the precipitation anomalies in a, with blue (red) for values greater (less) than  $+(-) 0.2 \text{ mm/day}$ .